NMR Study of the Dynamics of Hydrogen in the Cluster Compounds $Th_6H_xBr_{15}$ ($x = 5, 7$)

Thomas P. Braun,*,† Michael Mehring,‡ and Arndt Simon†

Contribution from the Max-Planck-Institut für Festkörperforschung, Heisenbergstrasse 1, D-70569 Stuttgart, Germany, and 2. Physikalisches Institut, Universität Stuttgart, Stuttgart, Germany

Received November 29, 1995[⊗]

Abstract: The complex dynamical behavior of the disordered hydrogen atoms in the recently discovered cluster compounds $Th_6H_7Br_{15}$ and $Th_6H_5Br_{15}$ has been investigated by means of ^1H solid state NMR. Two different modes of motion can be identified. At temperatures above 250 K the spin−lattice relaxation is dominated by a thermally activated *inter*cluster jump process with an activation energy of about 4200 K (360 meV). The emergence of this process results in an abrupt line narrowing of the NMR spectrum at 270 K. Down to the lowest measured temperature of 80 K a local *intra*cluster mode is effective. The low-temperature proton spin−lattice relaxation time is analyzed on the basis of a first principle stochastic model for $Th_6H_7Br_{15}$. A dynamically disordered and phonon assisted tunneling process is proposed for the low-temperature dynamics.

Introduction

The recently discovered compound $Th_6H_7Br_{15}$[1,2] offered the first example of a cluster in which the number of interstitial (hydrogen) atoms exceeds the number of metal atoms. As further investigations showed, this compound can be reversibly dehydrogenated at 875 K to yield the compound $Th_6H_5Br_{15}$.[3] This unique pair of compounds has been studied in detail as a model system for octahedral cluster compounds with variable electron count. According to our analysis of the chemical bonding and regarding the reversibility of the synthesis, these compounds seemed to be good candidates to study the nature of the disorder observed in the hydrogen sublattice. In particular the time scale of the expected dynamics of the hydrogen atoms seemed to be of general interest.

The structure of the heavy elements in the cluster compounds $Th_6H_7Br_{15}$ and $Th_6H_5Br_{15}$ corresponds to the structure of Nb_6F_{15}.[4] Octahedral Th_6Br_{12} clusters with twelve bromine atoms above all edges are connected via linear bridges by an additional six bromine atoms above all vertices of the octahedron according to $Th_6Br_{12}Br_{6/2}$. Two distinct primitive nets interpenetrate to build a body centered cubic cell.

According to neutron diffraction experiments on $Th_6D_7Br_{15}$[1,2] and $Th_6D_5Br_{15}$,[3] the hydrogen atoms are disordered on eight positions slightly above the centers of all triangular faces of the octahedron. One such $[Th_6H_xBr_{18}]^{3-}$ cluster unit is shown in Figure 1 emphasizing the arrangement of the hydrogen atoms in a cube.

The observed lengths of the edges of the hydrogen atom cube of 205.2(5) pm for $Th_6D_7Br_{15}$ and 188(5) ppm for $Th_6D_5Br_{15}$ are surprisingly short considering the fact that the hydrogen atoms in these compounds are best described as hydridic. However, for both compounds these values represent the distances between the average positions of the hydrogen atoms.

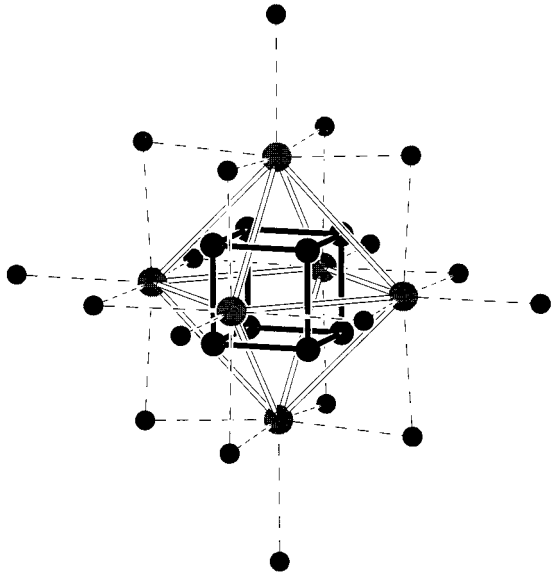

Figure 1. The structure of the $[Th_6H_xBr_{15}]^{3-}$ cluster unit. For $x = 5$ and 7 the corners of the hydrogen atom cube are occupied to $^5/_8$ and $^7/_8$, respectively.

In the individual cluster units only seven and five positions are occupied, respectively, and it can be assumed that the actual positions of the hydrogen atoms deviate from the crystallographic cubic symmetry giving rise to somewhat longer distances in the relaxed structures particularly in the case of $Th_6D_5Br_{15}$.

Nevertheless, these distances are significantly shorter than the hydrogen−hydrogen distances in related compounds. For other ternary hydride halides the shortest reported distances are 231 pm in $TbBrD_2$[5] and 227 pm in ZrBrD.[6] If compared to binary hydrides, the observed values are much shorter than, e.g., in ThH_2 (252 pm),[7] ZrH_2 (222 pm),[7] or HfH_2 (218 pm)[8] and

† Max-Planck-Institut für Festkörperforschung.
‡ 2. Physikalisches Institut, Universität Stuttgart.
[⊗] Abstract published in *Advance ACS Abstracts,* July 1, 1996.

(1) Böttcher, F.; Simon, A.; Kremer, R. K.; Buchkremer-Hermanns, H.; Cockcroft, J. K. *Z. Anorg. Allg. Chem.* **1991**, *598/599*, 25−44.
(2) Simon, A.; Böttcher, F.; Cockcroft, J. K. *Angew. Chem.* **1991**, *103*, 79−80.
(3) Braun, T. P.; Simon, A. *Chem. Eur. J.* **1996**, *2*, 131−135.
(4) Schäfer, H.; von Schnering, H. G.; Niehues, K. J.; Nieder-Vahrenholz, H. G. *J. Less.-Common Met.* **1965**, *9*, 95.
(5) Mattausch, H.; Simon, A.; Ziebeck, K. *J. Less-Common Met.* **1985**, *113*, 149.
(6) Wijeyesekera, S. D.; Corbett, J. D. *Solid State Commun.* **1985**, *54*(7), 657−60.
(7) Rundle, R. E.; Shull, C. G.; Wollan, E. O. *Acta Crystallogr.* **1952**, *5*, 22.

S0002-7863(95)04016-9 CCC: $12.00

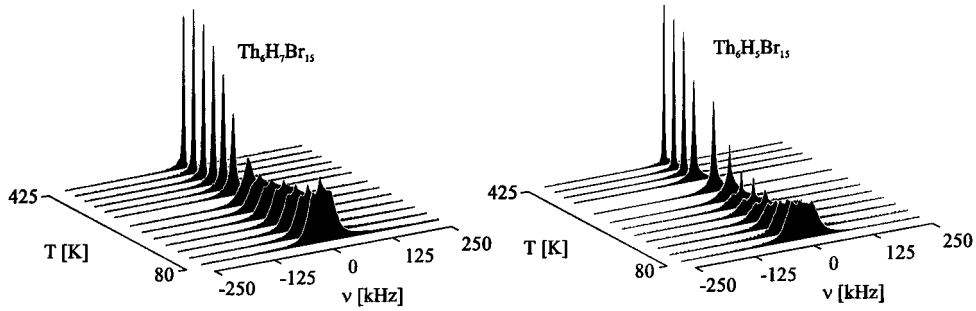

Figure 2. ^{1}H NMR spectra for $Th_6H_7Br_{15}$ (left) and $Th_6H_5Br_{15}$ (right) in the temperature range from 80 (front) to 425 K (back).

also shorter than in the "mixed valence" compound Th_4H_{15} (252 pm).[9,10] They rather compare to the shortest[11] distances found in UH_3 (206 pm)[12,13] or HoH_3 (204 pm).[14]

The refinement of the neutron diffraction data yields a structure model integrated over space and time. Thus the "statistical" disorder of the hydrogen atoms could be due to either the superposition of differently oriented clusters or a dynamic disorder of the hydrogen atoms on each cluster. Dynamic disorder of a hydrogen atom in an octahedral metal cluster has been described earlier for $Zr_6Cl_{12}H_x$ (x proposed to be 1).[15] To be able to decide on the nature of the disorder in these compounds we recorded the ^{1}H solid-state NMR spectra and determined the longitudinal relaxation rates of the protons for both compounds in the temperature range from 80 to 425 K.

Experimental Section

NMR measurements were performed with a multipulse spectrometer. The magnetic field of 7.75 T (≙ 330 MHz) was supplied by a superconducting 9 T magnet (Bruker). The temperature was controlled by a constant stream of nitrogen cooled by an ITC thermocontrol unit (Oxford). To correct for imperfections in pulse widths and phases of the spectrometer, phase cycling procedures were applied to reduce artifacts due to ringing effects.

The spin−lattice relaxation rates were determined by the saturation recovery method. The pulse sequence consisted of ten saturation (90°) pulses separated by τ_s (τ_s was set to 200 μs for temperatures below 300 K and to 60 μs for temperatures above 300 K). The recovered magnetization of the sample was then detected by another 90° pulse after the time τ, τ being varied from 1 ms to 16.348 s. Two such sequences were separated by a 2-ms break. The lengths of the 90° pulses were determined experimentally for each temperature range. They varied in the range of 2.7 to 2.9 μs. The time dependence of the "recovered" magnetization $M_z(t) = a \exp(-T_1/t)$ was fitted using all data on the one hand and only the data points with $\tau_s > 256$ ms on the other for statistical reasons. Both fits yielded very similar results for T_1, and the average values were used for the further treatment of the data.

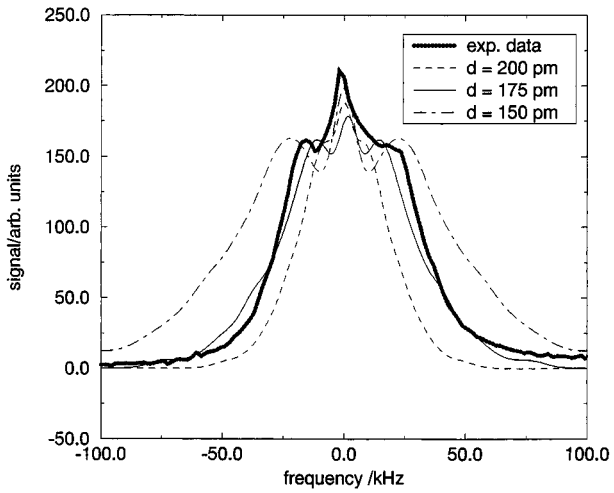

Figure 3. Experimental ^{1}H NMR spectrum and simulations (see text for details) for $Th_6H_7Br_{15}$ at 80 K.

Two samples of $Th_6H_7Br_{15}$ and $Th_6H_5Br_{15}$ were prepared according to (3) and about 250 mg have been sealed under helium in special ("water-free") quartz glass tubes of 5-mm diameter and approximately 25-mm length.

Results and Discussion

^{1}H Spectra. The spectra for $Th_6H_7Br_{15}$ and $Th_6H_5Br_{15}$ are represented in Figure 2. For both samples there is a quite abrupt narrowing of the resonance lines from 60 to 20 kHz at about 270 K. At higher temperatures the line width decreases further to about only 5 kHz at 425 K. This "motional narrowing" is a clear indication of dynamic behavior and proves that the disorder of the hydrogen atoms in these cluster compounds is dynamical even at room temperature.

Below 250 K the line width slowly increases toward lower temperatures to values of 70 and 80 kHz for $Th_6H_7Br_{15}$ and $Th_6H_5Br_{15}$, respectively. The line shapes of these low-temperature spectra differ significantly for the two samples.

A relatively sharp central peak above the broad base peak is characteristic for the spectra of $Th_6H_7Br_{15}$. The general shape of the spectrum recorded at 80 K can be reproduced by simulation. In the simulation calculation the dipolar Hamiltonian matrix for the interaction of the seven protons was diagonalized exactly. A subsequent "powder averaging" has been applied by the (statistically weighted) summation of all orientations of the sample with respect to the direction of the magnetic field.

The time-averaged arrangement of the hydrogen atoms is a cube with an edge length d as the only adjustable parameter. In Figure 3 we show the experimental ^{1}H NMR spectrum of $Th_6H_7Br_{15}$ at 80 K together with three simulations for $d = 150$, 175, and 200 pm.

The simulation with $d = 175$ pm comes closest to the experimental data, whereas the simulation for $d = 200$ pm is

(8) Sidhu, S. S. *Acta Crystallogr.* **1954**, *A7*, 447.
(9) Zachariasen, W. H. *Acta Crystallogr.* **1953**, *6*, 393.
(10) Mueller, M. H.; Beyerlein, R. A.; Jorgensen, J. D.; Brun, T. O.; Satterthwaite, C. B.; Caton, R. *J. Appl. Crystallogr.* **1977**, *10*, 79.
(11) For hydridic systems there are numerous data base entries of hydrogen−hydrogen distances below 200 pm. However, all of them are either "artificial" distances between partially occupied positions, in certain cases due to incorrect choice of space groups, or calculated from estimated hydrogen positions. There are no such distances confirmed by the refinement of neutron diffraction data of the respective deuterides.
(12) Grundle, R. E. *J. Am. Chem. Soc.* **1951**, *73*, 4172.
(13) Bartscher, W.; Boeuf, A.; Caciuffo, R.; Fournier, J. M.; Kuhs, W. F.; Rebizant, J.; Rustichelli, F. *Solid State Commun.* **1985**, *53*, 423.
(14) Mansmann, M.; Wallace, W. E. *J. Phys.* **1964**, *25*, 454.
(15) Chu, P. J.; Ziebarth, R. P.; Corbett, J. D.; Gerstein, B. C. *J. Am. Chem. Soc.* **1988**, *110*, 5324−9.
(16) The "activation" energies for the three temperature ranges (T > 320 K, 120 K > T > 320 K, and 120 K > T) are 90, 25, and 7 meV for $Th_6H_7Br_{15}$ and 78, 13, and 2 meV for $Th_6H_5Br_{15}$.

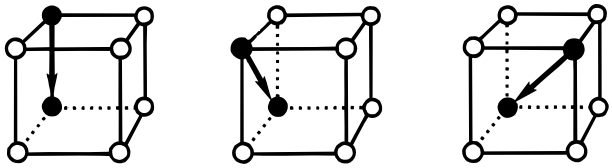

Figure 4. Possible *intra*cluster jumps for the hydrogen atoms in $Th_6H_xBr_{15}$ (from left to right): *ortho*, *meta*, and *para*.

definitely off. The distance of 175 pm is unrealistically low and not consistent with the value of 205 pm as determined by neutron diffraction. However, there is an important distinction between the two methods: In the diffraction experiment the (mean) *positions* of the scattering centers are determined, while the NMR experiment detects averages over *distances* (r^{-3}). If oscillations are allowed to take place, the positions will not be affected—at least if harmonic oscillations are assumed. Since the dipolar interaction scales with r^{-3} these oscillations generate a much stronger interaction for shorter distances and the averaged distances appear to be shorter. Model calculations show this effect is significant but cannot fully explain the difference of almost 15%.

A closer inspection reveals a significant asymmetry in all the spectra. Since geometrical asymmetries are explicitly corrected for and the spectra for solely dipolar coupled species must be symmetrical, there must be an additional contribution. Indeed there are three bromine atoms at distances of 286 pm near each proton. They introduce non-cubic local symmetry (*m.m*2) and contribute both an additional dipolar symmetric and a higher order indirect quadrupolar broadening which leads to an asymmetric line shape. In order to fully account for all the details of the spectrum the chemical shift anisotropies must be known (including their orientation) and all other nuclei (with their distribution of isotopes) have to be included. This task is beyond the scope of this contribution which concentrates on the dynamics of the hydrogen atoms.

For $Th_6H_5Br_{15}$ the situation is even more complicated. In contrast to only one distinct form in $Th_6H_7Br_{15}$ there exist three different ordered isomers of symmetry C_{3v} (1×) and C_s (2×) in the case of $Th_6H_5Br_{15}$. They all differ in the relative strengths of the dipolar couplings. Since a quantitative simulation is not possible even for the "simple" case of the cluster with seven protons, no attempts were made to calculate these spectra.

From the spectra alone it is evident that there are two different temperature regimes. Within both ranges the line width changes with temperature indicating that the hydrogen atoms are mobile. From the absolute values of the line widths it can be concluded that two distinct modes of motion are activated in the two different temperature regimes.

Relaxation Rates. As opposed to the strong and sharp change of the line widths the observed relaxation rates of $Th_6H_7Br_{15}$ and $Th_6H_5Br_{15}$ vary only slightly and rather smoothly in the range of 0.1 (at 80 K) to 0.8 s^{-1} (at 425 K) and 0.8 to 4.5 s^{-1}, respectively. When the data are plotted in an Arrhenius manner ($\ln(1/T_1)$ versus $1/T$) three "linear" temperature ranges (T > 320 K, 120 K > T > 320 K, and 120 K > T) can be identified. Interestingly, the "transition" temperatures are identical (within error) for both $Th_6H_7Br_{15}$ and $Th_6H_5Br_{15}$. The corresponding "activation" energies are unrealistically low for phononic processes[16] and have no physical meaning. The situation is rather complex and will be analyzed in the following by invoking dynamical disorder and phonon assisted tunneling.

For $Th_6H_7Br_{15}$ (one vacancy per hydrogen atom cube) there are only three distinct ways the vacancy can jump (see Figure 4). These are differentiated into a total of 21 in the case of three vacancies as in $Th_6H_5Br_{15}$. They differ in the relative number of nearest and second nearest neighbors both before and after the exchange. Additionally many jump possibilities lead to a different isomer than the starting one. Hence $Th_6H_7Br_{15}$ was chosen as a model for both compounds and analyzed in detail.

The key problem in the appropriate description of the dynamics of the hydrogen atoms in these compounds lies in the fact that two entirely different modes of motion are superimposed, namely *intra*- and *inter*cluster dynamics. Further complications arise from the fact that the maximum of the contribution of the *intra*cluster process to the spin−lattice relaxation rate and the onset of the *inter*cluster process almost coincide on the temperature scale. In the following model we assign the high-temperature regime of the spin−lattice relaxation to thermally activated jump processes between different cluster units (*inter*cluster process), whereas the low-temperature regime is governed by *intra*cluster dynamics. The total spin−lattice relaxation rate can therefore be expressed as

$$\frac{1}{T_1} = \left(\frac{1}{T_1}\right)_{\text{intra}} + \left(\frac{1}{T_1}\right)_{\text{inter}} \tag{1}$$

The high-temperature mode is characterized by an exponentially increasing relaxation rate following the simple relation

$$1/T_1 = A \exp(-E_A/T) \tag{2}$$

where E_A is the activation energy of the inter*cluster* hopping process. This corresponds to the slow-motion regime. The complete expression is obtained following Bloembergen, Purcell, and Pound (BPP)[17−19] as

$$\frac{1}{T_1} = \frac{2}{3}\Delta M_2 \left\{ \frac{\tau_{\text{inter}}}{1+\omega_0^2\tau_{\text{inter}}^2} + \frac{4\tau_{\text{inter}}}{1+4\omega_0^2\tau_{\text{inter}}^2} \right\} \tag{3}$$

where ΔM_2 is the change in the proton second moment (M_2) caused by intercluster hopping. The correlation time is expressed as a thermally activated process as

$$\tau_{\text{inter}} = (\tau_{\text{inter}})_0 \exp(E_A/T) \tag{4}$$

Its value can be estimated from the experimentally observed line width by using the relation $(\Delta M_2)^{1/2} = \pi \cdot \Delta\nu/(2 \ln 2)^{1/2}$ where the line width $\Delta\nu$ (full width at half height in units of hertz) corresponds to $\Delta\nu = 6 \times 10^4$ Hz. We can estimate the activation energy E_A from the line-narrowing mechanism which occurs at $T = 250$ K. By invoking the relation $\Delta M_2\tau^2 \simeq 1$ at the narrowing temperature we obtain $E_A = -T^* \ln\{(\Delta M_2)^{1/2}\tau_0\}$, where $T^* = 250$ K is the characteristic temperature where the line-narrowing occurs. When using a typical value of $(1/\tau_0)_{\text{inter}} \simeq 10^{12}$ s^{-1} for the phononic frequency we obtain $E_A \simeq 3900$ K (335 meV). This will be compared later with the values obtained from a complete simulation of the total relaxation rate where the values of E_A and $(1/\tau_0)_{\text{inter}}$ quoted here are taken as initial parameters. This completes the calculation of $1/T_1$ for the *inter*cluster jump process which determines the high-temperature area of the experimentally observed T_1 data (see Figure 5).

The remaining data resemble somewhat the BPP-like behavior, however with a slower decrease of the relaxation rate toward lower temperatures than on the high-temperature side of the

(17) Bloembergen, N.; Purcell, E. M.; Pound, R. V. *Nature* **1947**, *10*(4), 475−6.
(18) Bloembergen, N.; Purcell, E. M.; Pound, R. V. *Phys. Rev.* **1948**, *73*(7), 679−712.
(19) Abragam, A. *The Principles of Nuclear Magnetism*; Oxford University Press: Oxford, 1961.

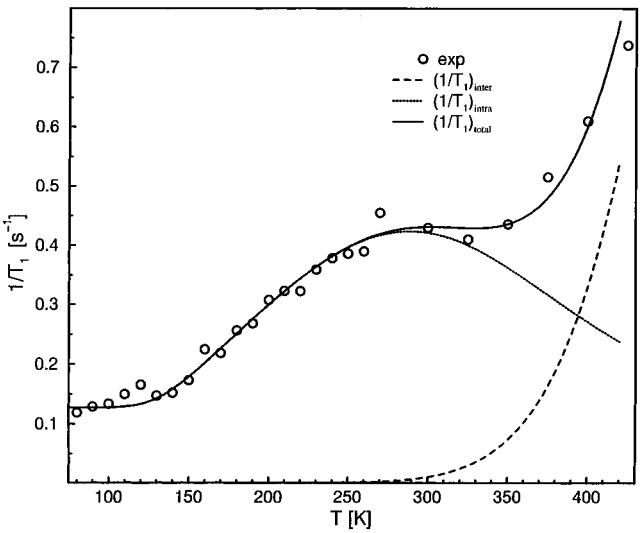

Figure 5. The proton relaxation rate $1/T_1$ versus temperature for $Th_6H_7Br_{15}$. The experimental data (dots) are compared with calculated relaxation rates (solid line) based on the models discussed in the text. *Intra*- ($1/T_{1_{intra}}$) and *inter*cluster ($1/T_{1_{inter}}$) contributions are plotted additionally.

BPP maximum. We will first analyze the residual data in the following by invoking an *intra*cluster vacancy motion. A stochastic model for this motion has been derived from first principles (see Appendix for details). According to this model the spin−lattice relaxation rate $1/T_1$ can be expressed using three effective (reduced) correlation times τ_i as:

$$\frac{1}{T_1} = \frac{1}{2}\sum_{i=1}^{3} V_i\{J_i(\omega_0) + 4\,J_i(2\omega_0)\} \tag{5}$$

where the prefactors V_i are effective interaction parameters. The reduced correlation times τ_i are nonlinear functions (for the exact definition see eq 15 in the Appendix) of the physically meaningful ("actual") correlation times τ_{ortho}, τ_{meta}, and τ_{para} for the respective site changes.

As it turns out a classical analysis of the data by using a Debye-type spectral density of the form

$$J_i(\omega_0) = \tau_i/(1 + (\omega_0\tau_i)^2) \tag{6}$$

together with an activated dynamics of the *intra*cluster dynamics is not sufficient to fit the experimental data.

Instead it is necessary to include dynamical disorder[20] combined with phonon-assisted tunneling[21] at low temperatures to account for the slow decrease of the relaxation rate at low temperatures. With these two additional assumptions the low-temperature longitudinal relaxation can be described on the basis of our first-principle stochastic model.

In Figure 5 we display the total proton relaxation rate $1/T_1$ versus temperature together with the experimental data for $Th_6H_7Br_{15}$. In order to demonstrate the different behavior of $(1/T_1)_{intra}$ and $(1/T_1)_{inter}$ we have plotted them additionally. We note the asymmetric behavior of $(1/T_1)_{intra}$ which is typical for disordered dynamics.

In this scenario, instead of three distinct correlation times for the three different site changes τ_{ortho}, τ_{meta}, and τ_{para} a *distribution* of correlation times is assumed for a given temperature following a Davidson−Cole[22] distribution that is characterized by an upper limit τ_{intra} ($0 < \tau \leq \tau_{intra}$) and a broadening parameter β ($0 \leq \beta \leq 1$):

$$g(\tau) = \frac{\sin(\beta\pi)}{\pi}\left(\frac{\tau}{\tau_{intra} - \tau}\right)^{\beta} \tag{7}$$

This distribution has a maximum at τ_{intra}. The resulting spectral density function can be expressed as[20]

$$J(\omega_0) = \frac{\sin[\beta \arctan(\omega_0\tau_{intra})]}{\omega_0[1 + (\omega_0\tau_{intra})^2]^{\beta/2}} \tag{8}$$

and reduces to the Debye-type formula if the broadening parameter β is set to 1. In this description eq 5 is simplified significantly since all three reduced correlation times τ_i are equal to 8 τ_{intra}. As a consequence the remaining prefactor $V = {}^1/_2\sum_i V_i$ has to be multiplied by the factor ${}^1/_8$ for the subsequent fit.

In order to allow for phonon-assisted tunneling at low temperatures we assume the following temperature dependence for the correlation time

$$(1/\tau)_{intra} = C_0 + C_1\exp(-E_A/T) \tag{9}$$

which was used by Punkinnen[21] in order to explain the phonon-assisted tunneling of methane molecules at low temperatures. Here the constant C_0 is connected with the energy difference of the top of the librational potential and the ground state while C_1 accounts for the fact that reorientation from the first librational state requires less energy than a reorientation from the ground state. Both quantities are given in units of s^{-1} and represent effective rates. The activation energy E_A represents the energy difference between the ground state and the first librational state.

Table 1. Parameters Used for the Simulation of the Relaxation Rates $(1/T_1)_{intra}$ According to Eqs 5, 8, and 9 and $(1/T_1)_{inter}$ According to Eqs 3 and 4 ($\omega_0 = 2 \times 10^9$ s^{-1})

$(1/T_1)_{intra}$	$(1/T_1)_{inter}$
$E_A = 1700$ K (147 meV)	$E_A = 4200$ K (360 MeV)
$C_0 = 8 \times 10^5$ s^{-1}	$1/\tau_0 = 1.5 \times 10^{12}$ s^{-1}
$C_1 = 3 \times 10^{11}$ s^{-1}	
$V = 1.5 \times 10^9$ s^{-2}	
$\beta = 0.2$	

The parameters obtained from the simulation shown in Figure 5 are summarized in Table 1. The refined values of E_A and $(1/\tau_0)_{inter}$ agree very well with the ones estimated from the analysis of the line width at the onset of the narrowing mechanism (see above).

The same temperature dependence could—in principle—be applied to the three "actual" correlation times τ_{ortho}, τ_{meta}, and τ_{para} used in the stochastical model. As it turns out there seems to be no unambiguous assignment of the parameter sets to the specific site change possibilities. Even the relative order of the three processes remains uncertain. A more detailed investigation at low temperatures is required in order to unravel these subtleties.

Conclusions

It could be firmly established from the longitudinal relaxation of both $Th_6H_7Br_{15}$ and $Th_6H_5Br_{15}$ that the disorder of the hydrogen atoms as observed in the neutron diffraction experiments is dynamic rather than static. Two different dynamical processes are distinguished. These are assigned to *inter*- and *intra*cluster motion.

The high-temperature process can be described as a thermally activated process with an activation energy of about 360 meV.

(20) Albayrak, C.; Zeidler, M.; Küchler, R.; Kanert, O. *Ber. Bunsenges. Phys. Chem.* **1989**, *93*, 1119.
(21) Punkinnen, M. *Phys. Rev. B* **1980**, *21*, 54.
(22) Davidson, D. W.; Cole, R. H. *J. Chem. Phys.* **1951**, *19*, 1484.

At the onset temperature of 250 K the corresponding correlation time can be estimated from the line width to about 6×10^{-6} s. This process has been assigned to *inter*cluster jumps causing a net transport of hydrogen atoms through the sample.

The assignment of the high-temperature process as a diffusion-like process is supported by chemical and structural considerations. The shortest distance between two hydrogen atoms of different cluster units is only 631 pm. A proposed jump along that path (the crystallographic [111] direction) is not hindered by the neighboring bromine atoms. The reversibility of the dehydrogenation of these compounds supports this assignment.

The low-temperature process on the other hand is assigned to *intra*cluster jumps. Even for the geometrically "simple" case of $Th_6H_7Br_{15}$ (with only one vacancy in a cube arrangement of hydrogen atoms) the quantitative analysis of the temperature dependence of the relaxation rates yields a rather complex model. Although the situation is too complex for a quantitative analysis for $Th_6H_5Br_{15}$, the qualitative results are also valid for this case. A distribution of correlation times best fits the observed longitudinal relaxation in this temperature range. The characteristic correlation time τ_{intra} is assumed to follow an activated behavior with an activation energy of about 150 meV. This value corresponds approximately to the difference between the first librational state and the ground state of the cluster. The Davidson−Cole parameter $\beta = 0.2$ hints at a rather wide distribution of correlation times. The correlation time at the BPP maximum (at 270 K), which appears as a plateau in the total relaxation rate, can be calculated from simple reasoning and should be of the order $1/\omega_0 = 5 \times 10^{-10}$ s. The calculated (average) value of 3.75×10^{-10} s agrees very well with that estimate.

The *intra*cluster dynamical processes are effective down to 80 K (the lowest temperature reached in this investigation) and with correlation times of 2.6×10^{-7} s (at 80 K) still quite fast, consistent with the proposed phonon-assisted tunneling mechanism. We remark that the associated energy compares rather well to activation energies of vibrations of similar systems as, e.g., in $Nb_6I_{11}H$ (135 meV)[23] or Th_4H_{15} (70 and 135 meV).[24]

Acknowledgment. Thanks are due to J. Gross for experimental support. We are also indebted to O. Kanert for discussions on disordered dynamics. We gratefully acknowledge financial support by the Fonds der Chemischen Industrie.

Appendix: Stochastic Model for the Relaxation in $Th_6H_7Br_{15}$

The spin−lattice relaxation rate $1/T_1$ in the case of homonuclear dipole−dipole interaction can be calculated from the spectral functions $j_{kq}(\omega)$:[25]

$$\frac{1}{T_1} = \frac{1}{2}\{j_{21}(\omega_0) + 4j_{22}(2\omega_0)\} \tag{10}$$

These spectral functions in turn can be expressed as the Fourier transform of a self-correlation function $g_q(t)$:

$$j_{2q}(\omega) = R\int_0^\infty (-1)^q g_q(t) e^{-i\omega t}\,dt \tag{11}$$

with

$$g_q(t) = \langle \delta A_{2q}(0)\delta A_{2-q}(t)\rangle - \langle A_{2q}\rangle\langle A_{2-q}\rangle \tag{12}$$

For a system with eight possible orientations (i.e. different positions of the vacancy) the self-correlation function can be defined as a function of the probability functions $P(n',n,t)$ (n,n': position of the vacancy) in the rotating frame by summing over all spin pairs (i,j):[19]

$$g_q(t) = \sum_{n,n'=1}^{8} P(n,t=0)\cdot P(n',n,t)\cdot\left\{\sum_{\substack{i<j\\ \neq n,n'}} A_{2q}(i,j)\cdot A_{2-q}(i,j) + \sum_{\substack{k\\ \neq n,n'\\ n\neq n'}}^{8} A_{2q}(k,n')\cdot A_{2-q}(k,n)\right\} - \sum_{n,n'=1}^{8} P(n,t=0)\cdot P(n',t=\infty)\cdot \left\{\sum_{\substack{i<j\\ \neq n,n'}} A_{2q}(i,j)\cdot A_{2-q}(i,j) + \sum_{\substack{k\\ \neq n,n'\\ n\neq n'}}^{8} A_{2q}(k,n')\cdot A_{2-q}(k,n)\right\} \tag{13a}$$

The functions $P(n',n,t)$ are defined as the probability that the vacancy has moved from position n (at $t = 0$) to position n' within the time t. Corresponding to the three different possible site changes (see Figure 4) on a cube there are only four distinct (the vacancy can also stay at position n for the time t) probabilities P_α (α = *ipso*, *ortho*, *meta*, *para*). Thus the equation defining $g_q(t)$ can be separated as a summation over the four different probability functions:

$$g_q(t) = P(n)\cdot\sum_\alpha m_\alpha\cdot(P_\alpha - P(n'))\cdot S_{2q}^\alpha \tag{13b}$$

where

$$S_{2q}^\alpha = \sum_{\substack{i<j\\ \neq n,n'}} A_{2q}(i,j)\cdot A_{2-q}(i,j) + \sum_{\substack{k\\ \neq n,n'\\ n\neq n'}}^{8} A_{2q}(k,n')\cdot A_{2-q}(k,n)$$

if the transition $n \rightarrow n'$ (with multiplicity m_α) is of type α.

The conditional probability functions P_α have been calculated analytically by a stochastic model. For each position n the time-dependent differential of the probability is given as the sum of all possible site changes that populate and depopulate this particular site. The time dependence is contained in characteristic correlation times τ_i associated with each of the site changes, *ortho*, *meta*, and *para*. The resulting system of eight differential equations can be solved for specified initial conditions. The resulting probability functions are:

$$P_{ipso} = {}^1/_8\{1 + e^{-t/\tau_1} + 3e^{-t/\tau_2} + 3e^{-t/\tau_3}\} \tag{14a}$$

$$P_{ortho} = {}^1/_8\{1 - e^{-t/\tau_1} - e^{-t/\tau_2} + e^{-t/\tau_3}\} \tag{14b}$$

$$P_{meta} = {}^1/_8\{1 + e^{-t/\tau_1} - e^{-t/\tau_2} - e^{-t/\tau_3}\} \tag{14c}$$

$$P_{para} = {}^1/_8\{1 - e^{-t/\tau_1} + 3e^{-t/\tau_2} - 3e^{-t/\tau_3}\} \tag{14d}$$

(23) Fitch, A. N.; Barrett, S. A.; Fender, B. E. F.; Simon, A. *J. Chem. Soc., Dalton Trans.* **1984**, 501−5.
(24) Miller, J. F.; Satterthaite, C. B.; Brun, T. O. Proc. Conf. *Neutron Scattering* **1976**, 529−534.
(25) Mehring, M. *Principles of High Resolution NMR in Solids*, 2nd ed.; Springer: Berlin, 1983; p 318.

Here the correlation times τ_i for the respective site changes have been combined to yield the effective correlation times

$$\frac{1}{\tau_1} = \frac{6}{\tau_{\text{ortho}}} + \frac{2}{\tau_{\text{para}}} \tag{15a}$$

$$\frac{1}{\tau_2} = \frac{4}{\tau_{\text{ortho}}} + \frac{4}{\tau_{\text{meta}}} \tag{15b}$$

$$\frac{1}{\tau_3} = \frac{2}{\tau_{\text{ortho}}} + \frac{4}{\tau_{\text{meta}}} + \frac{2}{\tau_{\text{para}}} \tag{15c}$$

With $P(n) = P(n') = {}^1/_8$ and the multiplicities $m_{\text{ipso}} = m_{\text{para}} = 8$, $m_{\text{ortho}} = m_{\text{meta}} = 24$ the correlation function becomes:

$$g_q(t) = \frac{1}{8}\Big\{ e^{-t/\tau_1}\cdot(S_{2q}^{\text{ipso}} - 3S_{2q}^{\text{ortho}} + 3S_{2q}^{\text{meta}} - S_{2q}^{\text{para}}) + e^{-t/\tau_2}\cdot(3S_{2q}^{\text{ipso}} - 3S_{2q}^{\text{ortho}} - 3S_{2q}^{\text{meta}} + 3S_{2q}^{\text{para}}) + e^{-t/\tau_3}\cdot(3S_{2q}^{\text{ipso}} + 3S_{2q}^{\text{ortho}} - 3S_{2q}^{\text{meta}} - 3S_{2q}^{\text{para}})\Big\} \tag{16}$$

The tensor elements $A_{2q}^{(n)}$ are defined (using SI units):

$$A_{2q}^{(n)} = -\frac{\mu_0}{4\pi}\gamma^2\hbar\left(\frac{24\pi}{5}\right)^{1/2}\sum_{i\neq j} r_{i,j}^{-3} Y_{2q}(\theta_{ij},\phi_{ij}) \tag{17}$$

with the normalized spherical harmonics $Y_{2q}(\theta_{ij},\phi_{ij})$.

To simulate the powder sample one has to average over all orientations of the magnetic field using the tabulated[26] reduced rotation matrices $d_{q_p q}^{(2)}(\theta)$:

$$\overline{A_{2q}(i,j)A_{2-q}(i,j)} = \sum_{q_1,q_2=-2}^{+2} A_{2q_1}(i,j)A_{2q_2}(i,j)\,\underbrace{\overline{d_{q_1,q}^{(2)}(\theta)d_{q_2,-q}^{(2)}(\theta)}}_{\theta = 0\ldots 2\pi}\,\underbrace{\overline{e^{-i\phi(q_1+q_2)}}}_{\phi = 0\ldots\pi}$$

With the factors

$$V_1 = {}^1/_8(S_{2q}^{\text{ipso}} - 3S_{2q}^{\text{ortho}} + 3S_{2q}^{\text{meta}} - S_{2q}^{\text{para}}) = -2.94\times 10^9\ \text{s}^{-2}$$

$$V_2 = {}^1/_8(3S_{2q}^{\text{ipso}} - 3S_{2q}^{\text{ortho}} - 3S_{2q}^{\text{meta}} + 3S_{2q}^{\text{para}}) = 6.48\times 10^9\ \text{s}^{-2}$$

$$V_3 = {}^1/_8(3S_{2q}^{\text{ipso}} + 3S_{2q}^{\text{ortho}} - 3S_{2q}^{\text{meta}} - 3S_{2q}^{\text{para}}) = 23.26\times 10^9\ \text{s}^{-2}$$

the longitudinal relaxation rate $1/T_1$ is expressed as a function of the three (reduced) correlation times τ_a, τ_b, and τ_c:

$$\frac{1}{T_1} = \frac{1}{2}\left\{ V_1\left(\frac{\tau_1}{1+\omega_0^2\tau_1^2} + \frac{4\tau_1}{1+4\omega_0^2\tau_1^2}\right) + V_2\left(\frac{\tau_2}{1+\omega_0^2\tau_2^2} + \frac{4\tau_2}{1+4\omega_0^2\tau_2^2}\right) + V_3\left(\frac{\tau_3}{1+\omega_0^2\tau_3^2} + \frac{4\tau_3}{1+4\omega_0^2\tau_3^2}\right)\right\} \tag{18}$$

JA954016E

(26) Buckmaster, H. A. *Can. J. Phys.* **1964**, *42*, 386−91.